Supporting Information for

Interaction of Supported Phospholipid Bilayers with Diamond Nanoparticles Non-Covalently Functionalized with a Cationic Polyelectrolyte

Thomas R. Kuech,[a,#] Nasim Ganji,[a,#] Caroline Anastasia,[b] Marco D. Torelli,[c] Eric. S. Melby,[a] Arielle C. Mensch,[c,d] Emily R. Caudill,[c] Ralf Zimmermann,[d] Robert J. Hamers,[c*] Joel A. Pedersen[a,c,e]

[a] Environmental Chemistry and Technology Program, University of Wisconsin, Madison, WI 53706, USA

[b] Department of Chemistry, Johns Hopkins University, Baltimore, MD 21218, USA

[c] Department of Chemistry, University of Wisconsin, Madison, WI 53706, USA

[d] Leibniz Institute of Polymer Research Dresden, Dresden, Germany

[e] Department of Environmental Health and Engineering, Johns Hopkins University, Baltimore, MD 21218, US

*Corresponding author

CONTENTS

Supplemental Experimental Section

Supplemental Tables

Supplemental Figures

Figure S1. Representative frequency and dissipation traces for formation of supported phospholipid bilayers from vesicles composed of 9:1 DOPC:DOPG followed by PAH-nanodiamond attachment as monitored by QCM-D

Figure S2. ζ-potentials of silica and supported lipid bilayers composed of DOPC and the indicated mass percentage of DOPG. The ζ-potentials were derived from streaming current measurements.

Figure S3. Representative QCM-D traces for PAH-DNP attachment to SiO_2 substrates at different NaCl concentrations.

Figure S4. Atomic force microscopy images of DOPC bilayers containing increasing amounts of DOPG before and after exposure to PAH-DNP. Bilayers were imaged after 20 min of PAH-DNP attachment. AFM images were taken at the same spot on each sample prior to particle introduction and after particle attachment and rinsing. Measurements were repeated in triplicate for all bilayers imaged. The height scale corresponds to the images in both columns. All scales bars are 2 μm.

SUPPLEMENTAL EXPERIMENTAL SECTION

Text S1: QCM-D Sensor Cleaning. SiO_2-coated QCM-D sensors (QSX 303, Biolin Scientific) were cleaned by sonicating them in a 2% (w/v) sodium dodecyl sulfate solution (10 min), rinsing alternatively with DI water and ethanol three times, drying with N_2 gas, and exposing them to ultraviolet light (185 and 254 nm) in a UV-ozone chamber (Bioforce Nanosciences UV/Ozone Procleaner) for 20 min to remove any trace organic compounds.

Text S2: AFM Image Analysis. Silicon nitride probes (DNP, Bruker) with a nominal force constant of 0.35 $N \cdot m^{-1}$ were employed. We acquired images of triplicate preparations of each bilayer type examined. The images were analyzed using ImageJ to assess the relative amount of particles present for the different conditions.[1–3] A color threshold was determined to select only the bright regions of the image (representing the PAH-DNP particles on the bilayer). A mask was created of these bright regions on the bilayer and from this mask we determined the number of pixels associated with the particles. This value was ratioed to the total number of pixels in the image (each image was 512×512 pixels) to give the fractional surface coverage of particles on the bilayers.

Text S3: Random Sequential Adsorption (RSA) Modeling. We calculated the expected jamming limit of particles on the silica substrate using a random sequential adsorption model (RSA) representing

each particle and its associated water by a truncated cone.[4] As a first approximation, we assumed a particle with a 15 nm core diameter and, based on the hydrodynamic diameter of the particles ($d_h \sim 29$ nm), 7 nm of water extending from the particle on each side, resulting in a cone with a base radius of 14.5 nm. We used a truncated cone of 16 nm height, assuming 1 nm of bound water above the particle.[5]

Table S1. Structures of phospholipids and polymer used to wrap diamond nanoparticles.

compound	abbreviation	structure
		phospholipids
1,2-dioleoyl-*sn*-glycero-3-phosphocholine	DOPC	
1,2-dioleoyl-*sn*-glycero-3-phospho-(1'-*rac*-glycerol)	DOPG	
		Polymer
poly(allylamine hydrochloride)	PAH	
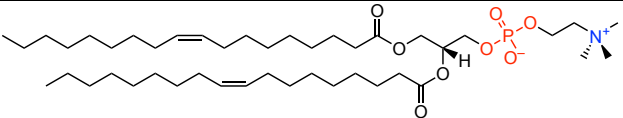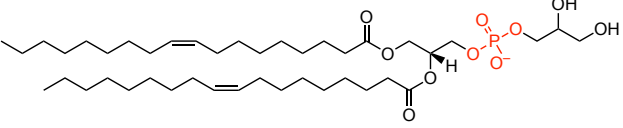
Table S2. Properties of small unilamellar phospholipid vesicles and supported phospholipid bilayers.[a]

vesicle composition		vesicles				supported lipid bilayers			
DOPC	DOPG	$d_{h,Z}$ (nm)	PDI[b]	$d_{h,n}$ (nm)	ζ (mV)	$-\Delta f_5/5$ (Hz)	ΔD_5 ($\times 10^{-6}$)	$\Delta\Gamma_{QCM-D}$ (ng·cm^{-2})	n
100%	–	128 ± 1	0.13 ± 0.01	89 ± 4	−2 ± 1	24.8 ± 0.7	0.446 ± 0.013	0.15± 0.06	25
90%	10%	113 ± 2	0.14 ± 0.009	72 ± 1	−15 ± 2	24.8 ± 0.4	0.446 ± 0.007	0.20 ± 0.07	32
80%	20%	90 ± 1	0.12 ± 0.007	58 ± 4	−25 ± 3	24.9 ± 0.3	0.448 ± 0.005	0.11 ± 0.03	20

[a] All experiments conducted in 0.1 M NaCl buffered to pH 7.4 with 0.01 M Tris. Abbreviations: $d_{h,n}$, number-average hydrodynamic diameter; $d_{h,Z}$, Z-average hydrodynamic diameter; n, number of replicates; PDI, polydispersity index; ζ, zeta-potential.
[b] The polydispersity index (PDI) is a measure of the distribution breadth and is derived from cumulants analysis as the ratio of the square of the second moment (variance) and to the mean decay constant.[6]

Table S3. Hydrodynamic diameters (d_h) and apparent ζ-potentials of PAH-DNPs.[a]

[NaCl] (M)	I (M)	κ^{-1} (nm)	Z-average d_h (nm)	PDI[b]	number mean d_h[c] (nm)	ζ-potential[d] (mV)
0.001	0.006	3.92	53 ± 2	0.37 ± 0.01	28 ± 1	45 ± 1
0.01	0.016	2.40	70 ± 1	0.30 ± 0.01	29 ± 1	43 ± 1
0.1	0.106	0.93	64 ± 2	0.37 ± 0.01	27 ± 1	34 ± 5

[a] All solutions were buffered to pH 7.4 with 0.01 M Tris. Abbreviations: d_h, hydrodynamic diameter; I, ionic strength; κ^{-1}, the Debye screening length

[b] The polydispersity index (PDI) is a measure of the distribution breadth and is derived from cumulants analysis as the ratio of the square of the second moment (variance) and to the mean decay constant.[6]

[c] The values at $I = 0.006$ and 0.016 M were statistically indistinguishable ($p > 0.05$); d_h at $I = 0.106$ was smaller than that at 0.016 M ($p = 0.0091$).

[d] The apparent ζ-potential at $I = 0.106$ was lower than at the other two ionic strength values ($p < 0.0003$).

Table S4. Changes in frequency and dissipation and acoustic surface mass density for maximal PAH polymer attachment to SiO₂ and supported phospholipid bilayers.[a]

ionic strength (M)	silica	DOPC	9:1 DOPC:DOPG	8:2 DOPC:DOPG
			$-\Delta f_5/5$ (Hz)	
0.006	1.6 ± 0.2	–	1.6 ± 0.1	–
0.016	2.5 ± 0.4	–	2.2 ± 0.4	–
0.106	3.5 ± 0.3	4 ± 0.3	4.6 ± 0.1	5 ± 1
			ΔD_5 ($\times 10^{-6}$)	
0.006	0.06 ± 0.01	–	0.10 ± 0.07	–
0.016	0.07 ± 0.04	–	0.12 ± 0.05	–
0.106	0.18 ± 0.05	9 ± 0.8	6.10 ± 0.23	0.4 ± 0.1
			$\Delta D_5/(-\Delta f_5/5)$ ($\times 10^{-6}$ Hz^{-1})	
0.006	0.04 ± 0.008	–	0.06 ± 0.044	–
0.016	0.03 ± 0.017	–	0.05 ± 0.025	–
0.106	0.05 ± 0.012	2.25 ± 0.20	1.32 ± 0.18	0.08 ± 0.02
			$\Gamma_{QCM\text{-}D}$ (ng·cm^{-2})[b]	
0.006	29 ± 4	–	30 ± 2	–
0.016	45 ± 8	–	40 ± 8	–
0.106	63 ± 5	72 ± 6	82 ± 8	91 ± 15

[a] PAH polymer concentration was 50 mg·L^{-1}. A dash indicates that the experiment was not performed for this solution condition.
[b] Values of $\Delta D_5/(-\Delta f_5/5)$ were $< 0.4 \times 10^{-6}$ Hz^{-1} justified the use of Sauerbrey equation with the exception of PAH attachment to DOPC and 9:1 DOPC:DOPG at an ionic strength of 0.106 M.[7,8] For these latter cases, a Kelvin-Voigt viscoelastic model was applied to estimate acoustic surface mass density.[9]

Table S5. Changes in frequency, dissipation and acoustic surface mass density for maximal PAH-DNP attachment to SiO₂ and supported phospholipid bilayers.

ionic strength (M)	silica	DOPC	9:1 DOPC:DOPG	8:2 DOPC:DOPG
			$-\Delta f_5/5$ (Hz)	
0.006	1.0 ± 0.2	104 ± 8	4 ± 1	4 ± 1
0.016	2.5 ± 0.4	128 ± 6	3.5 ± 0.2	2.9 ± 0.4
0.106	4.5 ± 0.2	172 ± 2	52 ± 6	11 ± 1
			ΔD_5 ($\times 10^{-6}$)	
0.006	0.18 ± 0.04	10 ± 2	0.4 ± 0.3	0.3 ± 0.2
0.016	0.19 ± 0.01	12 ± 1	0.3 ± 0.1	0.1 ± 0.1
0.106	0.27 ± 0.04	14 ± 1	6.8 ± 0.6	1.4 ± 0.3
			$\Delta D_5/(-\Delta f_5/5)$ ($\times 10^{-6}$ Hz^{-1})	
0.006	0.18 ± 0.05	0.05 ± 0.003	0.10 ± 0.079	0.08 ± 0.053

0.016	0.08 ± 0.01	0.04 ± 0.003	0.09 ± 0.029	0.03 ± 0.035
0.106	0.06 ± 0.01	0.04 ± 0.001	0.07 ± 0.005	0.06 ± 0.019
	$\Gamma_{QCM\text{-}D}$ (ng·cm^{-2})[a]			
0.006	18 ± 4	1870 ± 90	60 ± 20	60 ± 20
0.016	45 ± 8	2300 ± 110	63 ± 4	52 ± 8
0.106	65 ± 6	3110 ± 40	1800 ± 130	200 ± 20

[a] Values of $\Delta D_5/(-\Delta f_5/5)$ were $< 0.4 \times 10^{-6}$ Hz^{-1} justifying the use of Sauerbrey equation.[7,8]

Table S6. Attachment efficiencies (α_d) for PAH-DNP attachment to supported phospholipid bilayers.[a]

	attachment efficiencies (α_d)		
ionic strength (M)	DOPC	9:1 DOPC:DOPG	8:2 DOPC:DOPG
0.006	0.574 ± 0.031	0.017 ± 0.001	0.018 ± 0.001
0.016	0.943 ± 0.050	0.013 ± 0.001	0.014 ± 0.008
0.106	1.034 ± 0.056	0.004 ± 0.027	0.311 ± 0.017

[a] Attachment efficiencies were calculated as the ratio of the initial attachment rate to the indicated bilayer to the theoretical initial attachment rate to SiO$_2$ ($r_{d,SLB}/r_{d,SiO2}$). Initial rates for PAH-DNP are calculated from the second 30 s of PAH-DNP attachment to the indicated surface. The changes in frequency during the first 30 s is attributed to adsorption of free PAH, inequilibrium with bound PAH, in PAH-DNP solutions.
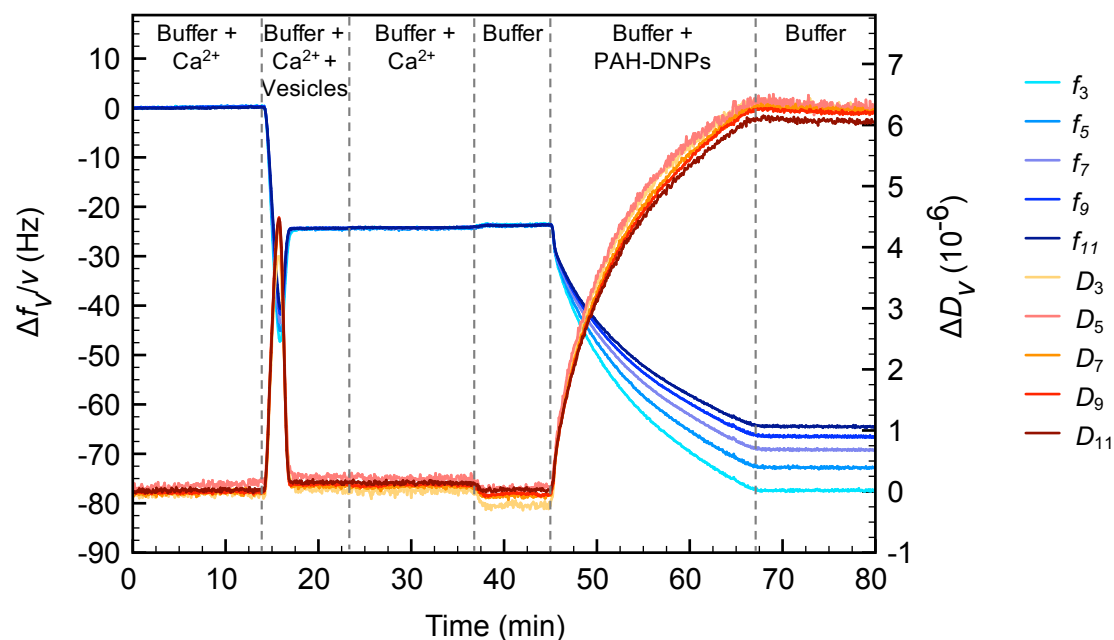
Figure S1. Representative frequency and dissipation traces for formation of supported phospholipid bilayers from vesicles composed of 9:1 DOPC:DOPG followed by PAH-

nanodiamond attachment as monitored by QCM-D. Abbreviations: ΔD_v, (orange), changes in energy dissipation; $\Delta f_v/v$ (blue), shift in frequency; v, number of the harmonic. Experiments were conducted at $I = 0.106$ M and pH 7.4 (0.01 M Tris).
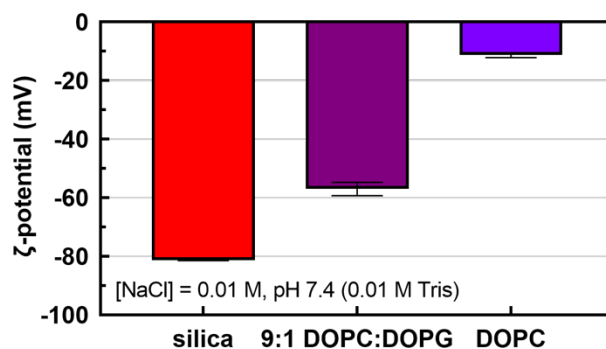
Figure S2. ζ-potentials of silica and supported lipid bilayers composed of DOPC and the indicated mass percentage of DOPG. The ζ-potentials were derived from streaming current measurements.
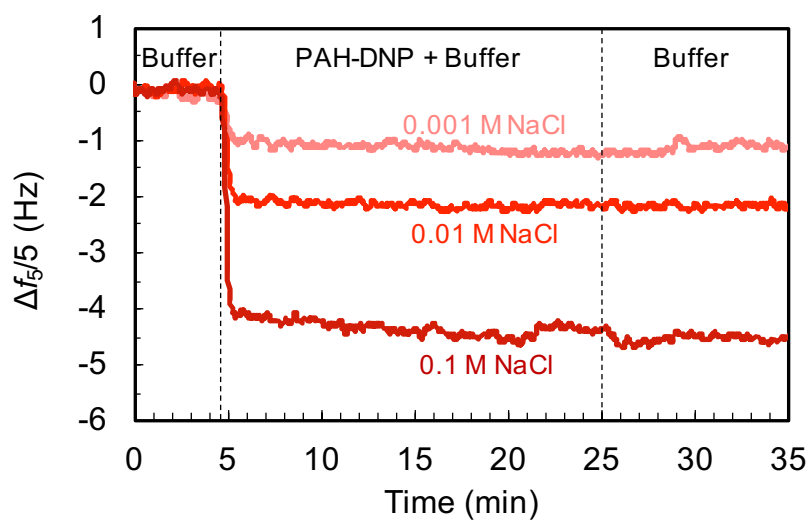
Figure S3. Representative QCM-D frequency traces (5th harmonic) traces for PAH-DNP attachment to SiO_2 substrates at different NaCl concentrations at pH 7.4 (0.01 M Tris).
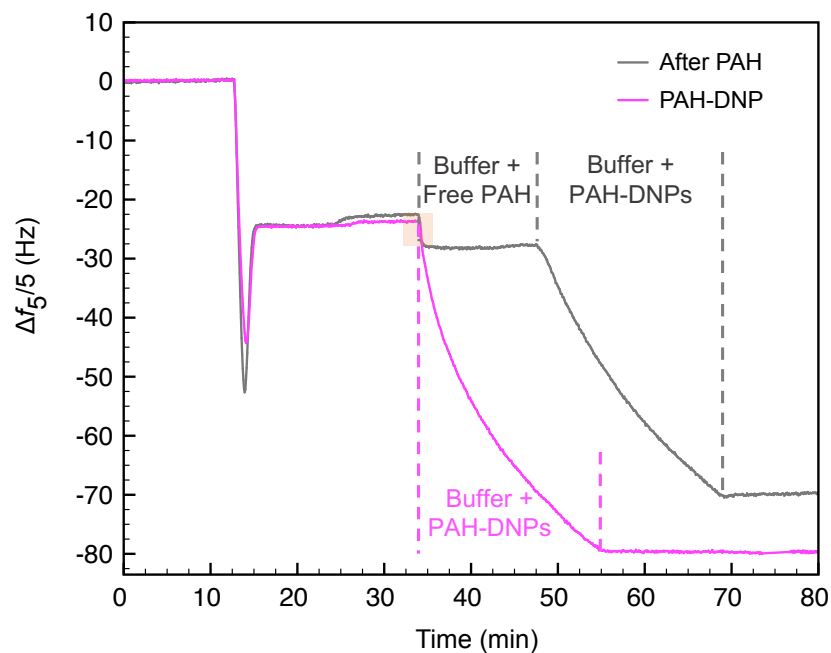
Figure S4. Representative frequency traces (5th harmonic) for formation of supported phospholipid bilayers from vesicles composed of 9:1 DOPC:DOPG followed by, PAH-DNP attachment (violet); and PAH-DNP attachment after PAH polymer (50 mg·L^{-1}) attained maximal attachment on the surface (grey). The change in frequency with respect to time due to the adsorption of PAH-DNP to the bilayer over the first 30 s being comparable to that for free PAH (red square). Experiments were conducted at I = 0.106 M and pH 7.4 (0.01 M Tris).
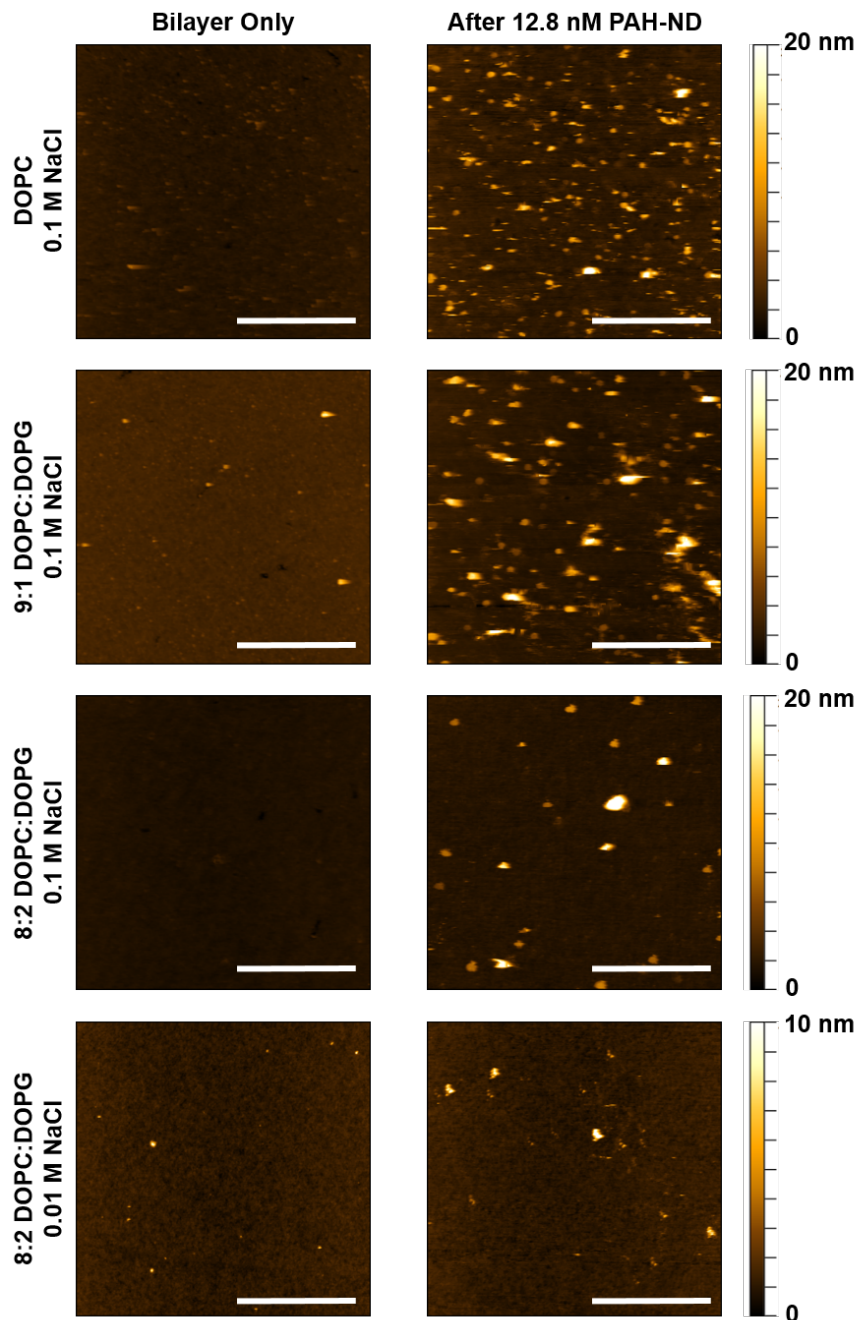
Figure S5. Atomic force microscopy images of DOPC bilayers containing increasing amounts of DOPG before and after exposure to PAH-DNP. Bilayers were imaged after 20 min of PAH-DNP attachment. AFM images were taken at the same spot on each sample prior to particle introduction and after particle attachment and rinsing. Measurements were repeated in triplicate for all bilayers imaged. The height scale corresponds to the images in both columns. Scales bars are 2 μm.

REFERENCES

1   M. D. Abràmoff, P. J. Magalhães and S. J. Ram, Image Processing with ImageJ, *Biophotonics Int.*, 2004, **11**, 36–41.

2   J. B. Sheffield, An introduction to ImageJ: A useful tool for biological image processing and analysis, *Microsc. Microanal.*, 2008, **14**, 898–899.

3   Rasband, W.S., ImageJ, https://imagej.nih.gov/ij/.

4   P. Bingen, G. Wang, N. F. Steinmetz, M. Rodahl and R. P. Richter, Solvation effects in the quartz crystal microbalance with dissipation monitoring response to biomolecular adsorption. A phenomenological approach, *Anal. Chem.*, 2008, **80**, 8880–8890.

5   Z. Adamczyk, *Particles at Interfaces*, Elsevier Ltd.: Netherlands, 2006, vol. 9.

6   R. Xu, *Particle Characterization: Light Scattering Methods*, Kluwer Academic Publishers, Dordrecht, 2002, vol. 13.

7   I. Reviakine, D. Johannsmann and R. P. Richter, Hearing What You Cannot See and Visualizing What You Hear: Interpreting Quartz Crystal Microbalance Data from Solvated Interfaces, *Anal. Chem.*, 2011, **83**, 8838–8848.

8   G. Sauerbrey, Verwendung von Schwingquarzen zur Wägung dünner Schichten und zur Mikrowägung, *Zeitschrift für Phys.*, 1959, **155**, 206–222.

9   M. V Voinova, M. Rodahl, M. Jonson and B. Kasemo, Viscoelastic Acoustic Response of Layered Polymer Films at Fluid-Solid Interfaces: Continuum Mechanics Approach, *Phys. Scr.*, 1999, **59**, 391–396.